



HAL
open science

Applications of an infrared thermography method for solid-liquid equilibria modeling of organic binary systems

Clément Mailhe, Fouzia Achchaq, Marie Duquesne

► To cite this version:

Clément Mailhe, Fouzia Achchaq, Marie Duquesne. Applications of an infrared thermography method for solid-liquid equilibria modeling of organic binary systems. *Thermochimica Acta*, 2020, 687, pp.1-9. 10.1016/j.tca.2020.178580 . hal-03166906

HAL Id: hal-03166906

<https://hal.inrae.fr/hal-03166906>

Submitted on 20 May 2022

HAL is a multi-disciplinary open access archive for the deposit and dissemination of scientific research documents, whether they are published or not. The documents may come from teaching and research institutions in France or abroad, or from public or private research centers.

L'archive ouverte pluridisciplinaire **HAL**, est destinée au dépôt et à la diffusion de documents scientifiques de niveau recherche, publiés ou non, émanant des établissements d'enseignement et de recherche français ou étrangers, des laboratoires publics ou privés.



Distributed under a Creative Commons Attribution - NonCommercial 4.0 International License

Applications of an infrared thermography method for solid-liquid equilibria modeling of organic binary systems

Clément Mailhé^{1*}, Fouzia Achchaq¹, Marie Duquesne².

¹ Université de Bordeaux, CNRS, I2M Bordeaux, Esplanade des Arts et Métiers, 33400 Talence, France

² Bordeaux INP, CNRS, I2M Bordeaux, ENSCBP, 16 avenue Pey Berland, 33600 Pessac, France

Abstract

The solid-liquid equilibria (SLE) modeling of fatty acids binary systems is known as a challenging topic. Due to their complex phase diagrams and to their inherent nature to polymorphism, the modeling of the solid-liquid equilibria of the fatty acids blends requires a significant amount of data obtained with numerous techniques. The infrared thermography method (IRT) proves to be an interesting alternative by providing large quantities of phase transitions data, including the potential detection of the polymorphic ones. In this work, the applicability of this method for SLE modeling is assessed based on two criteria: i) the accuracy of empirical and theoretical models is assessed in comparison with IRT data; ii) the polymorphic transition temperatures detected *via* IRT are used as inputs in a model using polymorphic transition enthalpies as adjusting parameters. Polymorphic transitions data is compared to literature and to DSC measurements to evaluate the reliability of IRT for polymorphic transitions detection and of the estimated enthalpies consistency.

Keywords: Solid-liquid equilibrium; Phase diagram; Polymorphism; Infrared thermography; Organic materials.

1. Introduction

Phase diagrams are very useful tools in material synthesis. Their assessment allows a deep understanding of the behaviors of materials and phase change dynamics. Their establishment through standard methods of calorimetry allows the gathering of experimental data required as inputs in equilibrium modeling [1-4]. Amongst them we can distinguish dynamic methods such as Differential Scanning Calorimetry (DSC) or X-Ray powder Diffraction (XRD) and static methods such as Scanning Electron Microscopy (SEM). The wide range of available methods arises from the variety of information they can provide. Their complementarity is a reason why a combination of methods is often found in studies aiming to assess the phase equilibria of systems of materials [5-7]. The use of multiple methods is actually required to fully and reliably establish a phase diagram. In [8-10] for instance, authors use several methods including some of the aforementioned ones to establish the phase diagrams of binary systems of fatty acids. Due to their large availability [11], their relatively low-cost [12], their renewable nature and their wide range of applications (food industry, pharmaceuticals, bio-fuel, thermal energy storage ...) [13], the study of fatty acids and bio-sourced compounds in general is an important research topic. A large scale study of such systems can be very time-consuming if an accurate and reliable phase

37 diagram is expected. In fact, phase diagrams obtained with standard methods usually include only 10 to
38 20 experimental datasets as individual experiments are to be performed for each sample. To accelerate
39 the screening process of materials and allow focusing calorimetry measurements on systems or
40 compositions of interest, an innovative method based on infrared thermography (IRT) was developed
41 [14]. This method has recently provided the estimation of complex phase diagrams of fatty acids binary
42 systems in a series of very short-time experiments [15-19]. In comparison with the phase diagrams
43 depicted in [8-10], presenting eutectic, peritectic, metatectic transitions and solid solubility domains, the
44 phase diagrams obtained using IRT show some inconsistent patterns including unsuspected transitions.
45 The latter are partly confirmed by DSC measurements. It is assumed that additional occurring transitions
46 might be of polymorphic nature as fatty acids are prone to such behavior as reported in [20, 21]. The
47 effect of such transitions on the liquidus line depiction can be accounted for in SLE modeling as reported
48 in [22-25] but it is usually left aside either because of insufficient data or because of an assumed
49 negligible influence. The form of the model presented in literature suggests that the IRT data regarding
50 polymorphic transitions temperatures could be used as inputs, leading to the model adjustments based
51 on polymorphic transitions enthalpies. The significant amount of gathered data as well as the potential
52 detection of polymorphic transitions indicates that IRT could be a tool of great interest for SLE modeling.

53 In that frame, the present study aims at assessing the potential applicability of IRT for SLE modeling
54 based on two main criteria. On the one hand, the accuracy of SLE models, relying on both predictive and
55 experimental-based approaches, is evaluated by comparison with the IRT data obtained for three binary
56 systems of fatty acids. On the other hand, the polymorphic transitions temperatures measured with IRT
57 are used as inputs in a SLE model using polymorphic enthalpies as fitting parameters. Both measured
58 temperatures and adjusted enthalpies are then compared with the literature values and with the DSC
59 measurements to confirm the applicability of IRT for polymorphic transition detection and its ability to
60 provide consistent enthalpy values.

61 2. Materials & Methods

62 2.1. Samples

63 Three systems of fatty acids are studied in this work: Capric acid + Lauric acid, Lauric acid + Palmitic acid
64 and Palmitic acid + Stearic acid. The phase diagrams of those systems are thoroughly studied in [8-10].
65 They are characterized by complex phase transitions, making the study of their solid-liquid equilibria a
66 challenging task. Several works aiming at characterizing the SLE of fatty acids systems can be mentioned
67 [26-31]. Although, they all hold the same purpose, considerably different results are presented. In fact, it
68 appears that experimental conditions play a major role in the determination of their phase diagrams. As
69 stated by Moreno et al. [20], fatty acids are prone to polymorphism which is heavily influenced by
70 crystallization kinetics and that can drastically alter the SLE of studied systems. Consequently, for the
71 comparison with the literature data hereafter, only results obtained with similar operating conditions are
72 considered. The pure compound properties from the remaining literature are still accounted for and are
73 compared with the properties obtained in this work in Table 1.

74 Table 1. Characteristics and thermal properties of the used chemicals at pressure $p = 0.1$ MPa.^a

	Capric acid	Lauric acid	Palmitic Acid	Stearic Acid
CAS number	334-48-5	143-07-7	57-10-3	57-11-4

Acronym		CA	LA	PA	SA
Formula		C ₁₀ H ₂₀ O ₂	C ₁₂ H ₂₄ O ₂	C ₁₆ H ₃₂ O ₂	C ₁₈ H ₃₆ O ₂
Molar mass (g/mol)		172.26	200.32	256.43	284.48
Melting enthalpy (J/mol)	This work	27 043	35 549	54 002	60 020
	[26-31]	23 430-29 400	32 640-39 470	46 020-54 830	57 740-68 443
Melting Temperature (K)	This work	303.45	316.45	335.23-336.43	342.30-342.56
	[26-31]	295.3-305.15	315.59-318.44	334.6-337.5	341.39-344.15
Supplier		Sigma-Aldrich	Sigma-Aldrich	Sigma-Aldrich	Sigma-Aldrich
Purity		99%	99%	>99%	>98,5%

75 ^a The melting enthalpy ΔH_m and melting temperature T_m are obtained from DSC measurements at
76 pressure $p = 0.1$ MPa following the protocol described in section 2.2.2. Standard uncertainties are $u(T_m) =$
77 0.5 K, $u(\Delta H_m) = 5\%$ and $u(p) = 10$ kPa. The molar mass and purity are indicated as provided by the supplier.

78 The melting enthalpies and temperatures obtained in this work are within range of literature values. It is
79 therefore assumed that the pure compound properties considered for SLE modeling in this work is
80 coherent and comparable to the SLE data extracted from literature.

81 2.2. Experimental data

82 The use of the IRT method for the study of phase change processes in organic materials has been
83 increasingly studied in the past years [32-34] as a way to efficiently contribute to the growing research
84 efforts in this field [8-10,13,26-31,35,36]. Its ability to rapidly estimate phase diagrams of systems of
85 organic materials including fatty acids has recently been proven in several works [14-19]. In this work,
86 the presented IRT results are validated based on phase transitions data extracted from literature and
87 from DSC measurements. We then rely only on the experimental data obtained using IRT to assess the
88 accuracy of the SLE model and to fit model parameters.

89 2.2.1. IRT

90 The estimated phase diagrams and liquidus lines are obtained using IRT according to the protocol
91 thoroughly described in [14]. Briefly, the method consists in monitoring the photonic flux emitted by
92 multiple samples with different molar compositions and submitted to a controlled heating ramp. A phase
93 transition in a sample is associated to heat exchanges, structural and morphological changes resulting in
94 an abrupt variation in the measured photonic flux. The signal variations are simultaneously identified for
95 all the samples throughout the heating experiment and allow consequently obtaining the estimated
96 phase diagram of each studied binary system. For each considered I-J binary system, 101 compositions
97 are studied ranging from 0 % I + 100 % J to 100 % I + 0 % J by 1 % increments approximately. The 1%
98 mentioned is actually given as an indication to have enough data to correctly depict the liquidus line. The
99 obtained phase diagrams then consist of 101 datasets.

100 For each composition, mixture batches of approximately 50 mg are prepared in aluminum weighing
101 pans. The appropriate amount of the compound I is weighed in powder form with a Mettler Toledo
102 weighing scale with a 0.03 mg accuracy. The content of the pan is melted at a temperature 5 °C above
103 the highest melting point of the two species and is then weighed again after it has completely
104 recrystallized. The compound J is added to the pan so that the total mass of two compounds allows
105 obtaining the objective molar fraction. It is then melted and weighed again after solidification to obtain
106 the actual molar percentage. Furthermore, with the LA+PA binary system for example, amongst the 101

107 compositions prepared, the maximum deviation between the objective molar percentage and the one
 108 obtained according to our weighing is around 0.045% (with an average deviation around 0.01%). The
 109 combined expanded uncertainty for the molar fraction is evaluated between 0.59 and 0.73% depending
 110 on purity which indicates that all prepared samples are at least within this range from the objective
 111 composition. From those negligible deviations, we can assume that each dataset obtained with the IRT
 112 method is given for the relevant composition.

113 2.2.2. DSC measurements

114 IRT measurements are followed with DSC experiments at selected compositions to validate the
 115 estimated phase diagrams. As getting 1 dataset at a time using this standard method is more time-
 116 consuming than getting 101 datasets with IRT, the validity of the phase diagram is generalized from local
 117 DSC measurements made at a few selected compositions. Two DSC heating ramps are programmed per
 118 sample: one at 1 °C/min matching the rate of the experiments using IRT and one at 0.3 °C/min to get
 119 more information on transitions that could be missed with a higher rate. The determination of the
 120 transition temperatures is performed according to the guidelines given in [37]. The interpolated onset
 121 temperature is considered as the transition temperature if a flat baseline can be obtained with the DSC
 122 curves. Otherwise peak temperatures are considered. In case the peak temperature must be considered,
 123 the results obtained with both the 1 °C/min and 0.3 °C/min rates are compared to make sure their
 124 difference is at least within the uncertainty range of the calorimeter. By doing so, we ensure that
 125 transition temperatures are consistent with a zero scanning rate experiment.

126 The experiments are performed with a DSC 131 provided by SETARAM and the data treatment is
 127 performed using the SETSOFT 2000 software. The DSC is calibrated using Gallium (Purity: 99.9999 %),
 128 Indium (Purity: 99.995 %), Tin (Purity: 99.999 %) and Lead (Purity: 99.999 %) to validate the results
 129 precision in the 30-330 °C temperature range.

130 Fatty acids samples of approximately 10 mg, and coming from the same batch used for the IRT
 131 experiment, are weighed using a Mettler Toledo scale with a 0.03 mg accuracy and are placed in open
 132 alumina crucibles.

133 2.3. SLE modeling

134 The thermodynamic model used for the modeling of the SLE of binary systems is given by Equation 1.
 135 This particular model, based on the fact that chemical potential of each substance in the solution is
 136 identical for the solid and liquid phases at equilibrium, has already been used and described in [22-25].

$$137 \ln\left(\frac{x_i \gamma_{L,i}}{z_i \gamma_{S,i}}\right) = \frac{\Delta H_{m,i}}{R} \left(\frac{1}{T_{m,i}} - \frac{1}{T}\right) + \frac{\Delta C_{p,i}}{R} \left(\frac{T_{m,i}}{T} - \ln\left(\frac{T_{m,i}}{T}\right) - 1\right) + \sum_{tr=1}^n \left(\frac{\Delta H_{tr,i}}{R} \left(\frac{1}{T_{tr,i}} - \frac{1}{T}\right) + \frac{\Delta C_{p,i}}{R} \left(\frac{T_{tr,i}}{T} - \ln\left(\frac{T_{tr,i}}{T}\right) - 1\right)\right) \quad (1)$$

137 with i identifying the species, x_i is the molar fraction of i in the liquid phase, z_i is the molar fraction of i in
 138 the solid phase, $\gamma_{L,i}$ is the activity coefficient of i in the liquid phase, $\gamma_{S,i}$ is the activity coefficient of i in
 139 the solid phase, R is the universal gas constant, $T_{m,i}$ is the melting temperature of i , T is the solid-liquid
 140 equilibrium temperature, $\Delta H_{m,i}$ is the melting enthalpy of i , $\Delta C_{p,i}$ is the difference between the liquid and
 141 solid heat capacities of i , $T_{tr,i}$ is a solid-solid transition temperature, $\Delta H_{tr,i}$ is the transition enthalpy
 142 associated to the latter transition.

143 This model is however more commonly found in the form given by Equation 2. This simplification comes
 144 from two main assumptions. First, it is assumed that the influence of the specific heat is negligible.
 145 Although, it was verified beforehand in our case that the specific heat difference is negligible compared
 146 to the latent heat of melting of fatty acids, it is a common practice especially for the SLE modeling of
 147 organic compounds. The second simplification considers the unity of the solid activity a_s ($a_s = z_i \gamma_{S,i}$). It
 148 arises from the choice to consider both components in the mixture as immiscible in the solid phase. It
 149 implies that solid solubility domains do not exist or that their range is limited.

$$\ln(x_i \gamma_{L,i}) = \frac{\Delta H_{m,i}}{R} \left(\frac{1}{T_{m,i}} - \frac{1}{T} \right) + \sum_{tr=1}^n \frac{\Delta H_{tr,i}}{R} \left(\frac{1}{T_{tr,i}} - \frac{1}{T} \right) \quad (2)$$

150 In addition, the previous formulation implies that the equilibrium occurs below a transition temperature.
 151 If we are in-between the melting temperature and the transition temperature, the right-hand part of
 152 Equation 2 should not be considered. In that case, we are left with Equation 3 which is the most
 153 commonly found in literature for SLE modeling [25, 30, 38]. A thorough explanation of the modeling
 154 process in the presence of polymorphic transitions is given in [22].

$$\ln(x_i \gamma_{L,i}) = \frac{\Delta H_{m,i}}{R} \left(\frac{1}{T_{m,i}} - \frac{1}{T} \right) \quad (3)$$

155 Moreover, binary systems of fatty acids differing by 2 or 4 carbon atoms are described in literature as
 156 having a complex phase diagram, specifically those including a peritectic transition. The methods to
 157 account for the effect of this reaction on the liquidus line have been studied [39-42] and consider the
 158 peritectic compound as the outcome of a stoichiometric chemical reaction between both I and J
 159 components in the mixture as represented in relation 4.



160 with v_I , v_J and v_P respectively the stoichiometric coefficients for the pure components I, J and the peritectic
 161 compound P.

162 From this consideration come the models depicted by Equations 5 and 6 which respectively, consider and
 163 exclude the effect of the polymorphic transitions. More details regarding their determination can be found
 164 in [39-41].

$$\sum_i \ln(x_i \gamma_{L,i}) = \sum_i v_i \left(\frac{\Delta H_{m,i}}{R} \left(\frac{1}{T_{m,i}} - \frac{1}{T} \right) + \sum_{tr=1}^n \left(\frac{\Delta H_{tr,i}}{R} \left(\frac{1}{T_{tr,i}} - \frac{1}{T} \right) \right) \right) - \frac{\Delta_r G^0}{RT} \quad (5)$$

165 With $\Delta_r G^0$ the Gibbs free molar energy of the peritectic reaction.

$$\sum_i \ln(x_i \gamma_{L,i}) = \sum_i v_i \left(\frac{\Delta H_{m,i}}{R} \left(\frac{1}{T_{m,i}} - \frac{1}{T} \right) \right) - \frac{\Delta_r G^0}{RT} \quad (6)$$

166 Although the model would be physically correct for a system in which a new compound is formed through
 167 the peritectic reaction, this transition actually often corresponds to a new crystalline structure from both
 168 compounds in a stoichiometric manner and not to the reaction itself. In this case, the value of the Gibbs
 169 energy of reaction is not representative of the actual reaction but just introduces an adjustable parameter

170 for the model which allows taking into account indirectly the peritectic transition in the depiction of the
171 liquidus line.

172 Solving the models described previously consists in a simple minimization procedure assuming that pure
173 compounds properties are known and that liquid activity coefficient and Gibbs energy of reaction if needed
174 are also known. If at least the melting enthalpies and temperatures of pure compounds are pre-required for
175 SLE modeling, the liquid activity coefficients, Gibbs energy of reaction and polymorphs properties are often
176 unknown. Different cases then arise for their determination.

177 Two approaches are possible for the evaluation of the liquid activity coefficient. Either experimental data is
178 used to fit the value or a predictive method is employed. The first approach is widely used for SLE modeling
179 and many methods exist such as the Margules-3-suffix, NRTL, Wilson or UNIQUAC [41]. Mostly used in
180 combination with the model presented in Equation 3, they aim at determining coefficients allowing the
181 computation of the liquid activity coefficient as a function of the molar fraction, the temperature and the
182 known pure compound properties. In this study, the Margules-3-suffix method is used to assess its efficiency
183 when fitted to the large amount of data provided by IRT. This method is combined to the model described in
184 Equations 3 and 6. This method provides a pair of coefficient a_{12} and a_{21} computed through Equation 7. The
185 Margules-3-suffix method was chosen as it is widely used for the SLE modeling of fatty acids and shows good
186 performances [23, 25, 30].

$$\begin{cases} RT \ln \gamma_{L,I} = (a_{12} + 3a_{21})(1 - x_1)^2 - 4a_{21}(1 - x_1)^3 \\ RT \ln \gamma_{L,J} = (a_{12} - 3a_{21})x_1^2 + 4a_{21}x_1^3 \end{cases} \quad (7)$$

187 with a_{12} and a_{21} the Margules coefficients, x_1 the molar fraction of the compound I and $\gamma_{L,I}$ and $\gamma_{L,J}$ the
188 liquid activity coefficient of I and J respectively.

189 The second method used in this work is the UNIFAC-Dortmund method which is based on group
190 contribution and is extensively discussed in [43]. It allows predicting the values of liquid activity coefficients
191 from the knowledge of pure compound properties and composition. This approach is particularly useful for
192 the simple binary systems as it is able to provide a liquidus line without the need for experimental data. In
193 our case, the presence of the peritectic transition implies fitting at least the Gibbs energy of reaction with
194 the experimental data. However the liquidus lines depicted by either Equation 2 or 3 could theoretically be
195 computed predictively assuming that polymorphic transitions are known beforehand.

196 As extensively discussed in [40] the solving process implies the consideration of regions defining which
197 equation to use for the liquidus line depiction. In fact, the determination of the Gibbs energy of reaction
198 requires to be fitted to experimental data. This adjustment implies, as mentioned, the identification of the
199 area in the liquidus affected by the peritectic reaction. In addition and as discussed previously, fatty acids are
200 characterized by numerous polymorphs [20,21]. Including polymorphic transitions in the model implies the
201 addition of new regions. In fact, as stated in [22] and as explained previously, one should use either Equation
202 2 or Equation 3 depending on the temperature as the pure compounds properties change according to
203 which polymorph is present. The detail of this process is given in [22]. Those polymorphic transitions are
204 challenging to characterize even with standard methods which is why they tend to be neglected in SLE
205 modeling. However, if the IRT method manages to provide polymorphic transition temperatures, then it
206 would be possible to use polymorphic transition enthalpies as fitting parameters. An estimation could be
207 provided for this thermal property assuming that the model assumptions are valid (negligible influence of

208 the specific heat and immiscibility in the solid phase). As explained by Maximo et al. [22], the form of the
209 model depicted by Equation 1-6 is intrinsically right if we are to use the polymorphic transition enthalpies as
210 adjusting parameters. Consequently, and as explained, adjusted values can be considered as coherent
211 approximations if and only if model assumptions are valid. Therefore, to avoid the confusion between the
212 actual polymorphic transition enthalpies and the adjusted parameters, ΔH_{tr} will be referred as ΔH_{calc} in the
213 results hereafter.

214 3. Results

215 For the 3 studied systems, the estimated phase diagram using IRT is plotted together with the DSC
216 measurements performed for the selected compositions. Both IRT and DSC data are available as
217 Supplementary material.

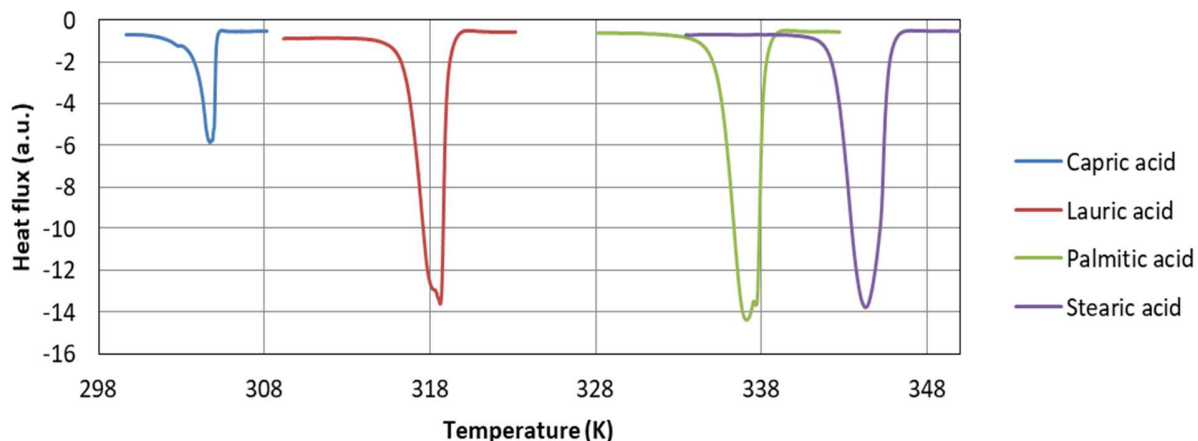
218 The liquidus line composed of IRT data points is compared to three SLE models. One uses the Margules-
219 3-suffix method for liquid activity coefficient computation. Its form is based on Equations 3 and 6. The
220 two remaining models use the UNIFAC-Dortmund method for liquid activity coefficient computation.
221 One is based on Equations 3 and 6 and the other on Equations 2 and 5. The latter, taking into account
222 the polymorphic behavior of fatty acids, uses the transition temperatures provided by the IRT method as
223 input. In this case, as the liquid activity coefficient calculation is predictive, the adjusting parameters are
224 the enthalpies of polymorphic transitions. The transition temperatures obtained with IRT are compared
225 with the known values from literature. The computed enthalpy values are also compared to the typical
226 ones for each fatty acid.

227 The accuracy of the models is made based on the comparison of their absolute average deviation (AAD)
228 calculated using Equation 8.

$$AAD = \sum_k \frac{|T_{k,IRT} - T_{k,calc}|}{T_{k,IRT} \times n} \times 100 \quad (8)$$

229 with $T_{k,IRT}$ the liquidus line temperature obtained using IRT for the sample k , $T_{k,calc}$ the liquidus line
230 temperature for the sample k computed using the SLE model and n the number of samples studied using the
231 IRT method.

232 Before presenting the results, one should be aware that pure fatty acids are known to present
233 polymorphic transitions very close to the melting temperature as seen in Figure 1 showing the DSC
234 thermograms of 4 pure fatty acids. Excluding the stearic acid, the double peaks are also observed in
235 literature [8-10,25] and have nothing to do with the impurities as the same results have been obtained
236 for different samples of the same materials. Besides, the impurity ratio of the purchased compounds is
237 very low (~1%). The melting enthalpy measured using our DSC is most likely the sum of the melting
238 enthalpy and of the polymorphic transition enthalpy occurring slightly before the melting point.
239 Although our DSC measurements do not corroborate the occurrence of this polymorphic transition for
240 the stearic acid, literature does [20]. Consequently for all studied compounds a polymorphic transition is
241 considered slightly below the melting point to account for its effect. From the DSC thermograms, it is
242 also expected that the computed polymorphic transition enthalpies be rather low in comparison with the
243 melting one.

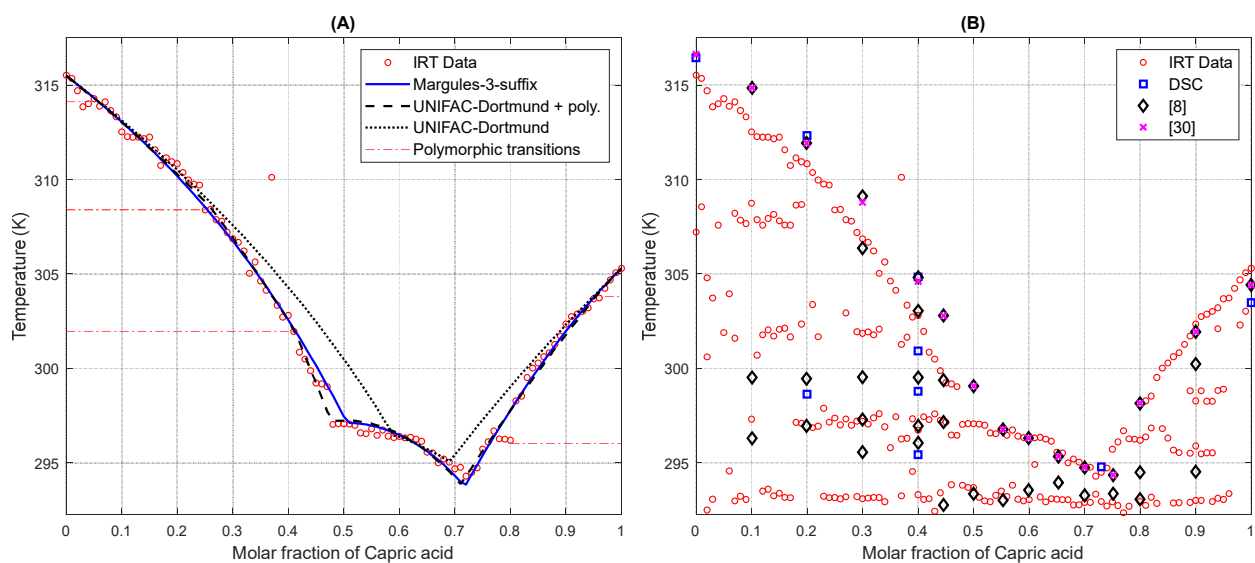


244
245
246

Fig. 1. DSC thermograms of the 4 pure studied fatty acids.

247 3.1. Capric acid - Lauric acid

248 Figures 2A and 2B respectively show the liquidus line depiction of the SLE models in comparison with the
249 IRT data and the CA+LA phase diagram estimated using the IRT method, DSC measurements and phase
250 transitions data extracted from [8, 30].



251
252
253

Fig. 2. (A) Liquidus line depiction of SLE models in comparison with IRT data; (B) CA+LA phase diagram estimated using the IRT method and DSC measurements.

254 As can be seen in Figure 2A, both models using the Margules-3-suffix method and the one accounting for
255 polymorphism provide a good fit with the IRT data. The purely predictive model based on the UNIFAC-
256 Dortmund method appears here to progressively deviate from the experimental liquidus line. If we
257 observe Figure 2B, we notice that the estimated phase diagram using the IRT method is sensibly different
258 from the one depicted in [8, 30]. Two transitions above the peritectic transition (in the 0%CA-25%CA and
259 0%CA-40%CA ranges respectively) are detected on the side rich in LA, that are neither fully confirmed by

260 DSC measurements or literature. On the side rich in CA, one additional transition (in the 80%CA-100%CA
 261 range) above the eutectic transition appears in comparison with literature. On the exception of those
 262 transitions, a fairly good agreement between experimental results from literature, DSC measurements
 263 and the ones obtained using the IRT method is obtained. The polymorphism of CA and LA and of fatty
 264 acids in general has not been widely studied. In fact, no polymorphism has yet been observed for CA but
 265 on the other hand, [44] introduces a polymorphic transition for the LA occurring around 308 K, which is
 266 consistent with the one detected using the IRT method.

267 The values of the different parameters for each used model as well as their relative accuracies are listed
 268 in Table 2.

269 Table 2. Parameters and accuracies of the models for the CA+LA binary system at pressure $p=0.1$ MPa. ^b

UNIFAC-Dortmund + polymorphism					Margules-3-suffix		UNIFAC-Dortmund
AAD (%)					AAD (%)		AAD (%)
0.12					0.13		0.33
$\Delta_r G^0$ (kJ/mol)					$\Delta_r G^0$ (kJ/mol)		$\Delta_r G^0$ (kJ/mol)
-1.22					-1.50		-0.52
CA: T_{tr} (K)		LA: T_{tr} (K)			a_{12} (kJ/mol)	a_{21} (kJ/mol)	
303.72	296.33	314.12	308.32	301.97	-1.85	-0.43	
CA: ΔH_{calc} (kJ/mol)		LA: ΔH_{calc} (kJ/mol)					
2.46	3.91	1.09	7.48	6.60			

270 ^b Standard uncertainties u are $u(T_{tr}) = 1.54$ K and $u(p) = 10$ kPa.

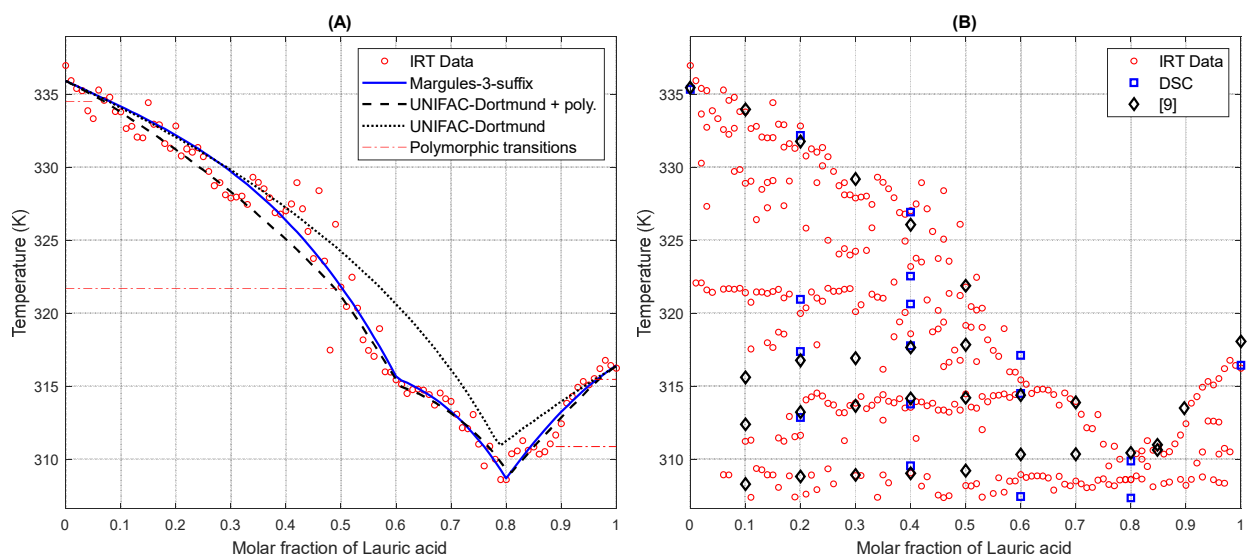
271 with T_{tr} the considered polymorphic transitions temperatures, whose value is taken as the average
 272 temperature of the IRT measurements, ΔH_{calc} the fitted polymorphic transition enthalpy, $\Delta_r G^0$ the
 273 adjusted value of the Gibbs energy of reaction for the peritectic transition, a_{12} and a_{21} the Margules
 274 adjusting coefficients.

275 The average absolute deviation obtained using the Margules-3-suffix method and for the one using the
 276 UNIFAC-Dortmund method and accounting for polymorphism is very close with even a slight advantage
 277 for the latter. Regarding the values of the enthalpy of polymorphic transitions, a comparison is only
 278 possible for documented transitions with measured enthalpies. The values obtained for the polymorphic
 279 transitions occurring close to the melting temperatures are rather low with 2.46 kJ/mol for the CA and
 280 1.09 kJ/mol for the LA, as expected from Figure 1. A polymorphic transition is detected using the IRT
 281 method around 308.32 K on the side of the phase diagram rich in LA. This transition is also documented
 282 in [44] but the value of its enthalpy is not indicated. A later study in [20], gives enthalpies of polymorphic
 283 transitions for other fatty acids with the same type of polymorphs. The values are 6.4 and 7.6 kJ/mol for
 284 the MA and PA, respectively. The value computed with our model is 7.48 kJ/mol which can be considered
 285 as a reasonable estimation. In [8-10], the phase diagrams of fatty acids binary systems presented by the
 286 authors are characterized by metastable and solid solubility domains whose actual occurrence is

287 arguable. The presence of these domains was in fact assumed based on the detection by DSC of
 288 horizontal transitions which are consistent with our measurements whether obtained by IRT or DSC.
 289 However, the gathered IRT data go against their assumptions and the existence itself of these domains is
 290 questionable. Consequently, undocumented transitions are considered as polymorphic in this work as a
 291 first approach, in order to include the effect of transitions such as the one detected at 296.33 K and
 292 301.97 K on the liquidus line. An in-depth study of their nature *via* other techniques (XRD for instance) is
 293 however expected. The SLE modeling of this binary system is also made in [30] using the Margules-3-
 294 suffix method and based on 15 data points obtained by DSC. The average absolute deviation measured
 295 by the authors is 0.12 % and the Margules parameters are evaluated at -1.60 kJ/mol for a_{12} and -1.30
 296 kJ/mol for a_{21} . As for the Gibbs energy of reaction, it is estimated at -1.20 kJ/mol. We notice that the
 297 model fit based on 101 data points obtained using the IRT method is as accurate as the one obtained for
 298 15 DSC measurements, which is highly encouraging for the potential use of the IRT method for SLE
 299 modeling. Although the model parameters are comparable and in the same range, they need to be
 300 nuanced as they highly depend on the pure compound properties considered and on their purity.

301 3.2. Lauric acid – Palmitic acid

302 Figures 3A and 3B respectively show the liquidus line depiction of the SLE models in comparison with the
 303 IRT data and the LA+PA phase diagram estimated using the IRT method, DSC measurements and phase
 304 transitions data extracted from [9].



305
 306 Fig. 3. (A) Liquidus line depiction of SLE models in comparison with IRT data; (B) LA+PA phase diagram
 307 estimated using the IRT method and DSC measurements.

308 Regarding the respective accuracies of the models in comparison with IRT data, the same conclusions as
 309 for the previous systems can be drawn. Indeed, from Figure 3A and Table 3, we see that both fitted
 310 models are relatively accurate in comparison with the predictive one. The latter presents significant
 311 deviations and cannot even depict the effect of the peritectic reaction on the liquidus line. We also
 312 notice that, even for experimentally fitted methods, the accuracy is lower than in the previous case. This
 313 loss in accuracy could be associated to the slight scattering of IRT data points in the 30%LA-50%LA range.

314 It however does not affect the overall phase diagram as the amount of data compensates for this local
 315 deviation.

316 As can be seen in Figure 3B, the phase diagram obtained using the IRT method is relatively consistent
 317 with results from DSC measurements or extracted from literature [9]. Although an horizontal transition
 318 occurring around 317 K between 10%LA-90%PA and 50%MA-50%PA could not be detected with certainty
 319 using the IRT method, another one around 312 K is detected and is confirmed by our DSC measurement
 320 (available in the Supplementary material). The latter can be associated to a polymorphic transition of PA
 321 similarly to the previous case. As for the LA, one polymorphic transition is considered with the same
 322 pattern as described in the previous system.

323 The values of the different parameters for each used model as well as their relative accuracies are listed
 324 in Table 3.

325 Table 3. Parameters and accuracies of the models for the LA+PA binary system at pressure $p=0.1$ MPa. ^c

UNIFAC-Dortmund + polymorphism				Margules-3-suffix		UNIFAC-Dortmund
AAD (%)				AAD (%)		AAD (%)
0.27				0.26		0.54
$\Delta_r G^0$ (kJ/mol)				$\Delta_r G^0$ (kJ/mol)		$\Delta_r G^0$ (kJ/mol)
-1.20				-2.19		-
LA: T_{tr} (K)		PA: T_{tr} (K)		a_{12} (kJ/mol)	a_{21} (kJ/mol)	
314.97	310.77	333.8	321.38	-3.44	-1.75	
LA: ΔH_{calc} (kJ/mol)		PA: ΔH_{calc} (kJ/mol)				
6.45	1.78	5.77	11.09			

326 ^c Standard uncertainties u are $u(T_{tr}) = 1.54$ K and $u(p) = 10$ kPa.

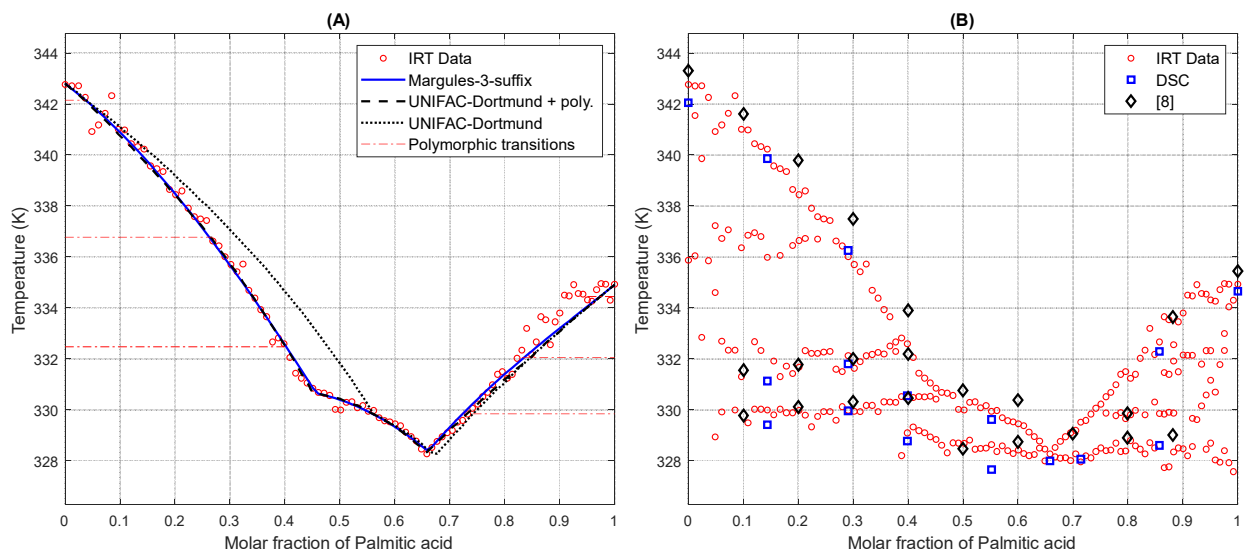
327 with T_{tr} the considered polymorphic transitions temperatures, whose value is taken as the average
 328 temperature of the IRT measurements, ΔH_{calc} the fitted polymorphic transition enthalpy, $\Delta_r G^0$ the
 329 adjusted value of the Gibbs energy of reaction for the peritectic transition, a_{12} and a_{21} the Margules
 330 adjusting coefficients.

331 The polymorphic transition detected above the eutectic line in the 85%LA-100%LA range is located at
 332 310.77 K. This temperature is not found elsewhere in literature and as stated previously, it may suggest
 333 that the nature of this transition is not polymorphic. In that case, the value of the computed enthalpy
 334 can only be considered as an adjusting parameter and does not bear any relevant physical meaning. A
 335 polymorphic transition around 321.38 K is also detected for the PA in the 0%LA-50%LA range using the
 336 IRT method. Literature reports the occurrence of a transition at 318.8 K in [21] while [20] report several
 337 ones at 316.7 K, 317.5 K and 324.7 K. Despite our transition temperature is encompassed by the
 338 literature ones, we cannot conclude with certainty on the polymorphic nature of this transition based
 339 solely on literature. Our DSC measurements however corroborate the transition detected using the IRT
 340 method. DSC data even appear to depict one around 317.5 K which is consistent with the polymorphic
 341 transition reported in literature but could unfortunately not be detected for enough samples to be

342 considered. The calculated enthalpy of polymorphic transition appears however to have been
343 overestimated. As for the enthalpies of the transitions close to the melting point, the 5.77 kJ/mol
344 computed for the PA can be considered low in comparison with the 54 kJ/mol measured for the melting
345 enthalpy but 6.45 kJ/mol appears to be slightly high. If the nature of the transition considered at 310.77
346 K is not polymorphic it may imply the presence of a solid solubility domain as suggested in [9]. If it is the
347 case, the assumptions of the model should be revisited or another way of accounting for this transition
348 should be investigated. The Margules-3-suffix method is also used in [30] to model the liquidus line of
349 this binary system based on 12 DSC measurements. The average absolute deviation measured by the
350 authors is 0.13 % and the Margules parameters are evaluated at -5.0 kJ/mol for a_{12} and -1.8 kJ/mol for
351 a_{21} . As for the Gibbs energy of reaction, it is estimated at -2.1 kJ/mol. If the Margules parameters are
352 rather close, we notice that the accuracy obtained based on the IRT results is not as accurate as in
353 literature. However, it should be mentioned that assessing the accuracy of the modeled liquidus line
354 based on only 12 experimental points is hazardous when depicting complex phase diagrams such as this
355 one as transitions and trend changes can easily be missed. We nevertheless notice that the modeled
356 liquidus line obtained in this work successfully depicts the experimental one as can be seen in Figure 3A.

357 3.3. Palmitic acid – Stearic acid

358 Figures 4A and 4B respectively show the liquidus line depiction of the SLE models in comparison with the
359 IRT data and the PA+SA phase diagram estimated using the IRT method, DSC measurements and phase
360 transitions data extracted from [8].



361

362 Fig. 4. (A) Liquidus line depiction of SLE models in comparison with IRT data; (B) PA+SA phase diagram
363 estimated using the IRT method and DSC measurements.

364 We can see from Figure 4A that both fitted models provide an estimated liquidus line almost not
365 dissociable from the experimental one obtained using the IRT method as corroborated by the average
366 absolute deviation computed in Table 5. The predicted liquidus line here fits rather well the right part of
367 the experimental liquidus line but still present deviations in the left part. The phase diagram obtained
368 using the IRT method as seen in Figure 4B is mostly consistent with DSC measurements and the one
369 depicted in [8]. In this case, the transition occurring around 332 K in the 10%PA-40%PA range and the

370 one occurring around 330 K in the 75%PA-90%PA range are both detected in [8] and the first is also
 371 verified in our DSC measurement (available in the Supplementary material). Another transition on both
 372 sides is detected consistently with the IRT method but could not be obtained with certainty using DSC.
 373 The four mentioned transitions are assumed in the model to be of polymorphic nature.

374 Table 4. Parameters and accuracies of the models for the PA+SA binary system at pressure $p=0.1$ MPa. ^d

UNIFAC-Dortmund + polymorphism						Margules-3-suffix		UNIFAC-Dortmund
AAD (%)						AAD (%)		AAD (%)
0.08						0.08		0.23
$\Delta_r G^0$ (kJ/mol)						$\Delta_r G^0$ (kJ/mol)		$\Delta_r G^0$ (kJ/mol)
-1.18						-1.19		-0.61
PA: T_{tr} (K)			SA: T_{tr} (K)			a_{12} (kJ/mol)	a_{21} (kJ/mol)	
334.26	332.17	329.9	341.68	336.72	332.89	-0.94	1.00	
PA: ΔH_{calc} (kJ/mol)			SA: ΔH_{calc} (kJ/mol)					
~ 0	-6.54	-1.87	6.11	2.52	-0.79			

375 ^d Standard uncertainties u are $u(T_{tr}) = 1.54$ K and $u(p) = 10$ kPa.

376 with T_{tr} the considered polymorphic transitions temperatures, whose value is taken as the average
 377 temperature of the IRT measurements, ΔH_{calc} the fitted polymorphic transition enthalpy, $\Delta_r G^0$ the
 378 adjusted value of the Gibbs energy of reaction for the peritectic transition, a_{12} and a_{21} the Margules
 379 adjusting coefficients.

380 Three polymorphic transitions are therefore considered in the model for the PA, one at 334.26 K, one at
 381 332.17 K and one at 329.9 K. In [20] and [45], a transition is reported to occur respectively around 331 K
 382 and 332.1 K which is consistent with the second one. Regarding the third one, we can once again not
 383 conclude on its polymorphic nature. In fact, we can see from Figure 4B that the IRT method also allows
 384 identifying a solid solubility domain. The presence of this domain suggests that this transition may not be
 385 polymorphic and its influence on the liquidus line depiction should be treated differently. As for the
 386 adjusted values of enthalpies of polymorphic transitions, they are not coherent with what should be
 387 expected. An explanation would be that as the predictive model is already rather accurate, either the
 388 influence of polymorphic transitions is negligible or, the melting point of the PA is misevaluated. In fact,
 389 from Figure 1 we see that the onset transition temperature is close to the melting point obtained using
 390 the IRT method whereas it actually represents the beginning of the polymorphic transition and not the
 391 melting point. It is likely then that the melting point is underestimated in this particular case. Regarding
 392 the SA, three polymorphic transitions are also considered, at 341.68 K, at 336.72 K and at 332.89 K. The
 393 occurrence of the first one is not supported by literature but the value of the adjusted enthalpy is
 394 coherent with our assumptions as 6.11 kJ/mol can be considered low in comparison with 60.02 kJ/mol.
 395 The second one is consistent with the one recorded in [45] at 337.1 K. It is also stated that its enthalpy of
 396 polymorphic transition is supposed to be low. This is also the case in our model with a value computed at
 397 2.52 kJ/mol. As for the last one, its polymorphic nature is uncertain but it could eventually be related to

398 the one present in [20] and occurring around 331.6 K. However the adjusted value is incoherent with the
399 expected ones, suggesting that either this transition is not polymorphic as assumed in [8] or that the
400 enthalpy of a previous transition has been miscalculated.

401 **4. Discussion**

402 The IRT method is an emerging method primarily aiming at the fast estimation of phase diagrams. For
403 numerous binary systems of organic materials, it has provided approached phase diagrams, consistent
404 with literature data and measurements made with standard calorimetric methods. Its main asset is its
405 capability to provide the phase transitions data of one system for a large amount of samples in a single
406 and short-time experiment. Due to its fundamentally different functioning principle, as detailed in [14],
407 the IRT method shows a capacity to possibly identify polymorphic transitions. Indeed, the detected
408 transitions have been compared with the polymorphic transitions found in literature for all studied
409 systems. This relatively good agreement between the values shows that the IRT method brings valuable
410 information for thermodynamic modeling as Equation 2 is commonly simplified to Equation 3 due to the
411 lacking data regarding polymorphism. However, the adjusted enthalpies of polymorphic transitions are
412 not always coherent with those collected from literature. Although the obtained values allow a good
413 depiction of the experimental liquidus line, it would be ideal to be able to use the model as a way of
414 estimating those thermodynamic properties. The model accounting for the polymorphic transitions for
415 the CA+LA and the PA+SA binary systems is particularly efficient due to the very accurate polymorphic
416 transitions detection. Besides, the computed enthalpies are consistent and in the range of literature
417 values, especially for LA and SA. We can see from Figures 2B and 4B that the phase diagrams obtained
418 using the IRT method is relatively simple and refined in comparison with the one from Figure 3B. Because
419 the left part of the phase diagram is less crowded with transitions, it is easier to accurately identify
420 transitions which may have led to a better depiction of the modeled liquidus line. On another note, the
421 authors show in [46] different DSC thermograms that could be associated to polymorphic transitions. It
422 states that depending on the thermal history of the sample and the monotropic or enantropic nature of
423 the system, polymorphs may or may not be noticeable and their representation on a thermogram can
424 have many aspects. It highlights the difficulties associated with the identification of polymorphic
425 transitions and the many ways in which they can affect SLE modeling. In addition, we can mention that
426 several recent works [47, 48] aim at improving DSC measurements for phase change materials,
427 emphasizing the challenge of phase transition characterization even with established standard methods.

428 From the large amount of data obtained with the IRT method, we see that the depicted line is coherent
429 and consistent with the DSC measurements. Despite a few local deviations, we have measured small
430 average absolute deviations which suggest that the IRT method is reliable for SLE modeling by providing
431 adequate experimental data and large datasets including, as we have seen, insightful information
432 regarding polymorphic transitions. However, for systems presenting areas dense in transitions such as
433 the LA+PA system, an improvement of the resolution of the IRT method may be needed for better
434 performances and to eventually be able to estimate thermal properties from SLE modeling.

435 **5. Conclusion**

436 The applicability of the IRT method as experimental data input for SLE modeling has been evaluated
437 upon assessing the performances of empirical and theoretical SLE models for the liquidus line depiction

438 of 3 binary systems of fatty acids (CA+LA, LA+PA and PA+SA). The IRT method is used to build
439 approached phase diagrams consisting of a large amount of datasets in a single experiment. The quantity
440 of obtained data is an advantageous feature to supply databases and is particularly interesting in SLE
441 modeling as it allows a better depiction of the equilibrium while making sure that every single region of
442 the liquidus line is accounted for. The detected transitions using the IRT method and not reported in
443 known phase diagrams have been compared to the polymorphic ones characterized in literature. For all
444 presented systems, we have been able to relate some detected transitions to polymorphic transitions
445 reported in literature. For the CA+LA and PA+SA systems, the computed enthalpies for those transitions
446 were in the range of the documented polymorphic ones. As for the remaining transitions, further works
447 are needed to fully identify their nature as neither literature nor our results allow any definitive
448 conclusion. Although the IRT method has shown to be able to detect a solid solubility domain which is an
449 interesting accomplishment for the estimation of complex phase diagrams, these results suggest that the
450 model assumptions may not be fully valid. Nevertheless, whether the detected transitions have been
451 successfully related to the polymorphism phenomenon or not, the model taking it into account has been
452 able to provide a liquidus line with a good accuracy. The IRT method should be applied to systems
453 presenting simpler phase diagrams and whose polymorphic behavior has been thoroughly studied in
454 order to definitely conclude on the benefits of using the IRT method in SLE modeling. Our results are
455 indeed encouraging as they suggest the IRT method could be used for other applications than providing a
456 full complex phase diagram in a single and fast experiment. Indeed, it could also allow for the
457 assessment of model assumptions beforehand and it may enable the incorporation of polymorphic
458 transition temperatures in the model in order to estimate the enthalpies of polymorphic transitions.

459 **Acknowledgements**

460 This work is carried out in the frame of SUDOKET project and is co-funded by the Interreg Sudoe
461 Programme through the European Regional Development Fund (ERDF). The authors acknowledge them
462 as well as the financial support of Region Nouvelle Aquitaine for subsidizing BioMCP project (Project-
463 2017-1R10209-13023). We also would like to thank CNRS for promoting the I2M Bordeaux - CICE
464 exchanges in the framework of the PICS PHASE-IR project.

465 **References**

- 466 [1] Campbell FC. Phase Diagrams: Understanding the Basics. ASM International. 2012.
467 [2] Institute for Materials Research (U.S.), National Measurement Laboratory (U.S.). Office of Standard
468 Reference Data, National Science Foundation (U.S.). Applications of Phase Diagrams in Metallurgy and
469 Ceramics: Proceedings of a Workshop Held at the National Bureau of Standards, Gaithersburg, Maryland,
470 January 10-12, 1977.
471 [3] Dubost B. Industrial applications and determination of equilibrium phase diagrams for light alloys.
472 Progress and prospects. Rev Met Paris. 1993;90(2):195-210.
473 [4] Yang Y, Bewlay BP, Chen S, Chang YA. Application of phase diagram calculations to development of
474 new ultra-high temperature structural materials. Transactions of Nonferrous Metals Society of China.
475 2007;17(6):1396-404.
476 [5] Chelouche S, Trache D, Pinho SP, Khimeche K. Experimental and modeling studies of binary organic
477 eutectic systems to be used as stabilizers for nitrate esters-based energetic materials. Fluid Phase
478 Equilibria. 2019;498:104-115.

479 [6] Chelouche S, Trache D, Pinho SP, Khimeche K, Mezroua A, Benziane M. Solid–Liquid Phase Equilibria,
480 Molecular Interaction and Microstructural Studies on (N-(2-ethanol)-p-nitroaniline + N-(2-acetoxyethyl)-
481 p-nitroaniline) Binary Mixtures. *Int J Thermophys.* 2018;39(11):129.

482 [7] Chelouche S, Trache D, Neves CMSS, Pinho SP, Khimeche K, Benziane M. Solid + liquid equilibria and
483 molecular structure studies of binary mixtures for nitrate ester’s stabilizers: Measurement and modeling.
484 *Thermochimica Acta.* 2018;666:197-207.

485 [8] Costa MC, Sardo M, Rolemberg MP, Coutinho JAP, Meirelles AJA, Ribeiro-Claro P, et al. The solid–
486 liquid phase diagrams of binary mixtures of consecutive, even saturated fatty acids. *Chemistry and
487 Physics of Lipids.* 2009;160(2):85-97.

488 [9] Costa MC, Sardo M, Rolemberg MP, Ribeiro-Claro P, Meirelles AJA, Coutinho JAP, et al. The solid–
489 liquid phase diagrams of binary mixtures of consecutive, even saturated fatty acids: differing by four
490 carbon atoms. *Chemistry and Physics of Lipids.* 2009;157(1):40-50.

491 [10] Costa MC, Rolemberg MP, Meirelles AJA, Coutinho JAP, Krähenbühl MA. The solid–liquid phase
492 diagrams of binary mixtures of even saturated fatty acids differing by six carbon atoms. *Thermochimica
493 Acta.* 2009;496(1-2):30-7.

494 [11] OCDE/FAO (2019). *OECD-FAO Agricultural Outlook 2019-2028*, OCDE Editions, Paris.

495 [12] Midgley C, LMC International. The market outlook for fatty acids. ICIS Pan American Oleochemical
496 Conference, October 2018.

497 [13] Maximo GJ, Costa MC, Coutinho JAP, Meirelles AJA. Trends and demands in the solid–liquid
498 equilibrium of lipidic mixtures. *RSC Adv.* 2014;4(60):31840-31850

499 [14] Palomo Del Barrio E, Cadoret R, Daranlot J, Achchaq F. Infrared thermography method for fast
500 estimation of phase diagrams. *Thermochimica Acta.* 2016;625:9-19

501 [15] Mailhé C, Duquesne M, Palomo del Barrio E, Azaiez M, Achchaq F. Phase Diagrams of Fatty Acids as
502 Biosourced Phase Change Materials for Thermal Energy Storage. *Applied Sciences.* 2019;9(6):1067

503 [16] Mailhé C, Duquesne M, Mahroug I, Palomo Del Barrio E. Improved infrared thermography method
504 for fast estimation of complex phase diagrams. *Thermochimica Acta.* 2019;675:84-91.

505 [17] Duquesne M, Mailhé C, Ruiz-Onofre K, Achchaq F. Biosourced organic materials for latent heat
506 storage: An economic and eco-friendly alternative. *Energy.* 2019;188:116067.

507 [18] Mailhé C, Duquesne M. A fast and low-cost dynamic calorimetric method for phase diagram
508 estimation of binary systems. *J Therm Anal Calorim.* 2020.

509 [19] Mailhé C, Duquesne M. Performance analysis of the infrared thermography method for complex
510 phase diagrams estimation. *J Therm Anal Calorim.* 2020.

511 [20] Moreno E, Cordobilla R, Calvet T, Cuevas-Diarte MA, Gbabode G, Negrier P, et al. Polymorphism of
512 even saturated carboxylic acids from n-decanoic to n-eicosanoic acid. *New Journal of Chemistry.*
513 2007;31:947-957.

514 [21] Gbabode G, Negrier P, Mondieig D, Moreno E, Calvet T, Cuevas-Diarte MÀ. Fatty acids
515 polymorphism and solid-state miscibility: Pentadecanoic acid–hexadecanoic acid binary system. *Journal
516 of Alloys and Compounds.* 2009;469(1):539-551.

517 [22] Maximo GJ, Costa MC, Meirelles AJA. The Crystal-T algorithm: a new approach to calculate the SLE
518 of lipidic mixtures presenting solid solutions. *Phys Chem Chem Phys.* 2014;16(31):16740-54.

519 [23] Maximo GJ, Aquino RT, Meirelles AJA, Krähenbühl MA, Costa MC. Enhancing the description of SSLE
520 data for binary and ternary fatty mixtures. *Fluid Phase Equilibria.* 2016;426(Supplement C):119-30.

521 [24] Lohmann J, Gmehling J. Solid–Liquid Equilibria for Seven Binary Systems. *J Chem Eng Data.*
522 2001;46(2):333-6.

523 [25] Maximo GJ, Carareto NDD, Costa MC, dos Santos AO, Cardoso LP, Krähenbühl MA, et al. On the
524 solid–liquid equilibrium of binary mixtures of fatty alcohols and fatty acids. *Fluid Phase Equilibria*.
525 2014;366:88-98.

526 [26] Zhang Z, Yuan Y, Zhang N, Cao X. Thermophysical Properties of Some Fatty Acids/Surfactants as
527 Phase Change Slurries for Thermal Energy Storage. *J Chem Eng Data*. 2015;60(8):2495–501.

528 [27] Kahwaji S, Johnson MB, Kheirabadi AC, Groulx D, White MA. Fatty acids and related phase change
529 materials for reliable thermal energy storage at moderate temperatures. *Solar Energy Materials and*
530 *Solar Cells*. 2017;167:109–20.

531 [28] Zhang J-J, Zhang J-L, He S-M, Wu K-Z, Liu X-D. Thermal studies on the solid–liquid phase transition in
532 binary systems of fatty acids. *Thermochimica Acta*. 2001;369(1):157–60.

533 [29] Cedeño FO, Prieto MM, Espina A, García JR. Measurements of temperature and melting heat of
534 some pure fatty acids and their binary and ternary mixtures by differential scanning calorimetry.
535 *Thermochimica Acta*. 2001;369(1):39–50.

536 [30] Costa MC, Rolemberg MP, Boros LAD, Krähenbühl MA, de Oliveira MG, Meirelles AJA. Solid–Liquid
537 Equilibrium of Binary Fatty Acid Mixtures. *Journal of Chemical & Engineering Data*. 2007;52(1):30-6.

538 [31] Schaake RCF, van Miltenburg JC, de Kruif CG. Thermodynamic properties of the normal alkanolic
539 acids II. Molar heat capacities of seven even-numbered normal alkanolic acids. *The Journal of Chemical*
540 *Thermodynamics*. 1982;14(8):771–8.

541 [32] Godin A, Palomo del Barrio E, Morikawa J, Duquesne M. Microscopic infrared thermography for fast
542 estimation of the thermal properties of thin films. *Journal of Applied Physics*. 2018;124(8):085111.

543 [33] Duquesne M, Godin A, Palomo del Barrio E, Daranlot J. Experimental analysis of heterogeneous
544 nucleation in undercooled melts by infrared thermography. *Quantitative InfraRed Thermography*
545 *Journal*. 2015;12(1):112-26.

546 [34] Godin A, Duquesne M, Palomo del Barrio E, Morikawa J. Analysis of crystal growth kinetics in
547 undercooled melts by infrared thermography. *Quantitative InfraRed Thermography Journal*.
548 2015;12(2):237-51.

549 [35] Duquesne M, Godin A, del Barrio EP, Achchaq F. Crystal growth kinetics of sugar alcohols as phase
550 change materials for thermal energy storage. *Energy Procedia*. 2017;139:315–21.

551 [36] Godin A, Duquesne M, del Barrio EP, Achchaq F, Monneyron P. Bubble agitation as a new low-
552 intrusive method to crystallize glass-forming materials. *Energy Procedia*. 2017;139:352–7.

553 [37] Boettinger WJ, Kattner UR, Moon K-W, Perepezko JH. Chapter 5 - DTA and heat-flux DSC
554 measurements of alloy melting and freezing. In: Zhao J-C, editor. *Methods for Phase Diagram*
555 *Determination*. Oxford: Elsevier Science Ltd; 2007. p. 151-221.

556 [38] Gmehling JG, Anderson TF, Prausnitz JM. Solid-Liquid Equilibria Using UNIFAC. *Ind Eng Chem Fund*.
557 1978;17(4):269-73.

558 [39] Barbosa DF, de Alcântara Pessôa Filho P. On the description of the liquidus line of systems
559 presenting peritectic reactions. *Fluid Phase Equilibria*. 2013;337:379-83.

560 [40] Rocha SA, Guirardello R. An approach to calculate solid–liquid phase equilibrium for binary mixtures.
561 *Fluid Phase Equilibria*. 2009;281(1):12-21.

562 [41] Slaughter DW, Doherty MF. Calculation of solid-liquid equilibrium and crystallization paths for melt
563 crystallization processes. *Chemical Engineering Science*. 1995;50(11):1679-94.

564 [42] Prausnitz JM, Lichtenthaler RN, and Gomes de Azevedo E. *Molecular Thermodynamics of Fluid-*
565 *Phase Equilibria*. Pearson Education, 1998.

- 566 [43] Gmehling J, Li J, Schiller M. A modified UNIFAC model. 2. Present parameter matrix and results for
567 different thermodynamic properties. *Ind Eng Chem Res.* 1993;32(1):178-93.
- 568 [44] Von Sydow E, *Ark. Kemi.* 1956;9: 231.
- 569 [45] Stenhagen E, Von Sydow E. The phase transitions in normal chain carboxylic acids with from twelve
570 up to and including twenty-nine carbon atoms between 30° and the melting point. *Ark. Kemi.*
571 1952;6(29):309-316
- 572 [46] Sato K, Kobayashi M. Structure, Stability and Crystal Growth of Polymorphs and Polytypes of Long-
573 Chain Aliphatic Compounds. In: Karl N, editor. *Organic Crystals I: Characterization.* Springer Berlin
574 Heidelberg; 1991. p. 65-108. (Crystals).
- 575 [47] Dumas JP, Gibout S, Cézac P, Franquet E. New theoretical determination of latent heats from DSC
576 curves. *Thermochimica Acta* 2018;670:92-106.
- 577 [48] Gibout S, Franquet E, Hailot D, Bédécarrats JP, Dumas JP. Challenges of the Usual Graphical
578 Methods Used to Characterize Phase Change Materials by Differential Scanning Calorimetry. *Applied*
579 *Sciences* 2018;8(1):66.